

# Probing the leptonic Dirac CP-violating phase in neutrino oscillation experiments

Tommy Ohlsson,<sup>1,\*</sup> He Zhang,<sup>2,†</sup> and Shun Zhou<sup>1,‡</sup>

<sup>1</sup>*Department of Theoretical Physics, School of Engineering Sciences,  
KTH Royal Institute of Technology, AlbaNova University Center, 106 91 Stockholm, Sweden*  
<sup>2</sup>*Max-Planck-Institut für Kernphysik, Saupfercheckweg 1, 69117 Heidelberg, Germany*

The discovery of leptonic CP violation is one of the primary goals of next-generation neutrino oscillation experiments, which is feasible due to the recent measurement of a relatively large leptonic mixing angle  $\theta_{13}$ . We suggest two new working observables  $\Delta A_{\alpha\beta}^m \equiv \max[A_{\alpha\beta}^{\text{CP}}(\delta)] - \min[A_{\alpha\beta}^{\text{CP}}(\delta)]$  and  $\Delta A_{\alpha\beta}^{\text{CP}}(\delta) \equiv A_{\alpha\beta}^{\text{CP}}(\delta) - A_{\alpha\beta}^{\text{CP}}(0)$  to describe the CP-violating effects in long-baseline and atmospheric neutrino oscillation experiments. The former signifies the experimental sensitivity to the leptonic Dirac CP-violating phase  $\delta$  and can be used to optimize the experimental setup, while the latter measures the intrinsic leptonic CP violation and can be used to extract  $\delta$  directly from the experimental observations. Both analytical and numerical analyses are carried out to illustrate their main features. It turns out that an intense neutrino beam with sub-GeV energies and a baseline of a few 100 km may serve as an optimal experimental setup for probing leptonic CP violation.

PACS numbers: 14.60.Pq, 11.30.Er

## I. INTRODUCTION

The phenomenon of neutrino oscillations in vacuum and matter can be described by six fundamental parameters: three lepton flavor mixing angles  $\{\theta_{12}, \theta_{13}, \theta_{23}\}$ , two neutrino mass-squared differences  $\{\Delta m_{21}^2, \Delta m_{31}^2\}$ , and one Dirac-type CP-violating phase  $\delta$ . Due to a number of elegant neutrino oscillation experiments in the past decades, both  $\{\theta_{12}, \Delta m_{21}^2\}$  and  $\{\theta_{23}, |\Delta m_{31}^2|\}$  have been measured with reasonably good accuracy [1]. Until recently, the smallest leptonic mixing angle  $\theta_{13}$  has been found to be relatively large in the Daya Bay [2] and RENO [3] reactor neutrino experiments. This great discovery enhances the capability of the next-generation experiments to pin down the neutrino mass hierarchy (i.e., the sign of  $\Delta m_{31}^2$ ) and eventually to determine the leptonic Dirac CP-violating phase.

An important question is how to characterize the leptonic CP-violating effects in neutrino oscillation experiments. For neutrino oscillations in vacuum, it is evident that the CP asymmetry, usually defined as  $A_{\alpha\beta}^{\text{CP}} \equiv P_{\alpha\beta} - \bar{P}_{\alpha\beta} \propto \sin \delta$  for  $\alpha \neq \beta$ , is well determined by  $\delta$ , where  $P_{\alpha\beta} = P(\nu_\alpha \rightarrow \nu_\beta)$  and  $\bar{P}_{\alpha\beta} = P(\bar{\nu}_\alpha \rightarrow \bar{\nu}_\beta)$  stand for the neutrino and antineutrino transition probabilities, respectively. For long-baseline neutrino oscillation experiments, however, matter effects [4, 5] can be significant and induce fake CP violation, since the Earth matter itself is CP asymmetric. In this case, the intrinsic CP violation due to  $\delta$  in  $A_{\alpha\beta}^{\text{CP}}$  is obscured by extrinsic CP violation caused by matter effects. On the other hand, one can determine  $\delta$  by just measuring the probabilities  $P_{\alpha\beta}$  as precisely as possible. In this case,

if one defines  $\Delta P_{\alpha\beta}^{\text{CP}}(\delta) \equiv P_{\alpha\beta}(\delta) - P_{\alpha\beta}(0)$ , the fake CP violation can be removed, since  $\Delta P_{\alpha\beta}^{\text{CP}}(\delta)$  vanishes for  $\delta = 0$ . Furthermore, it has been suggested [6] that  $\Delta P_{\alpha\beta}^m \equiv \max[P_{\alpha\beta}(\delta)] - \min[P_{\alpha\beta}(\delta)]$  can be utilized to quantify the experimental sensitivity to  $\delta$ , where the maximum and minimum are obtained by freely varying  $\delta$  in  $[0, 2\pi)$ . Both  $\Delta P_{\alpha\beta}^{\text{CP}}(\delta)$  and  $\Delta P_{\alpha\beta}^m$  have been studied in detail by using neutrino oscillograms of the Earth [7, 8].

Since the description of leptonic CP violation should reflect the difference between neutrinos and antineutrinos, we suggest  $\Delta A_{\alpha\beta}^{\text{CP}}(\delta) \equiv A_{\alpha\beta}^{\text{CP}}(\delta) - A_{\alpha\beta}^{\text{CP}}(0)$  and  $\Delta A_{\alpha\beta}^m \equiv \max[A_{\alpha\beta}^{\text{CP}}(\delta)] - \min[A_{\alpha\beta}^{\text{CP}}(\delta)]$  as working observables to signify the intrinsic CP violation and the experimental sensitivity to  $\delta$ . First, we make a general comparison among all five quantities (i.e.,  $A_{\alpha\beta}^{\text{CP}}$ ,  $\Delta P_{\alpha\beta}^{\text{CP}}$ ,  $\Delta P_{\alpha\beta}^m$ ,  $\Delta A_{\alpha\beta}^{\text{CP}}$ , and  $\Delta A_{\alpha\beta}^m$ ) and point out their advantages and disadvantages in describing leptonic CP violation. Then, we perform a detailed numerical study of them, and describe their main features by using approximate analytical formulas. Finally, we investigate the experimental setup that is optimal for the determination of  $\delta$ .

## II. MEASURES OF LEPTONIC CP VIOLATION

First of all, we briefly review the formulation of three-flavor neutrino oscillations in matter, which is relevant for long-baseline experiments. The flavor transition of neutrinos propagating in matter is governed by the effective Hamiltonian  $H_{\text{eff}} = H_v + V$ , where  $H_v = U \cdot \text{diag}(0, \Delta_{21}, \Delta_{31}) \cdot U^\dagger$  with  $\Delta_{21} \equiv \Delta m_{21}^2/2E$  and  $\Delta_{31} \equiv \Delta m_{31}^2/2E$  being the low and high oscillation frequencies and  $E$  is the neutrino energy. The matter potential is  $V \equiv \sqrt{2}G_F n_e \text{diag}(1, 0, 0)$ , where  $n_e$  is the electron number density. In the standard parametrization, the leptonic mixing matrix is  $U = O_{23}\Gamma_\delta O_{13}\Gamma_\delta^\dagger O_{12}$ , where  $O_{ij}$  denotes the rotation in the  $i$ - $j$  plane with an angle  $\theta_{ij}$  (for  $ij = 12, 13, 23$ ) and  $\Gamma_\delta = \text{diag}(1, 1, e^{i\delta})$  with

\*Electronic address: tohlsson@kth.se

†Electronic address: hzhang@mpi-hd.mpg.de

‡Electronic address: shunzhou@kth.se

$\delta$  being the leptonic Dirac CP-violating phase. Since  $V$  is invariant under any rotations in the 2-3 plane, one can transform to flavor basis  $(\nu_e, \tilde{\nu}_\mu, \tilde{\nu}_\tau)^T = U_{23}^\dagger(\nu_e, \nu_\mu, \nu_\tau)^T$  with  $U_{23} \equiv O_{23}\Gamma_\delta$  such that  $H'_{\text{eff}} = U_{23}^\dagger H_{\text{eff}} U_{23}$  is independent of  $\theta_{23}$  and  $\delta$  in this basis. The amplitude of neutrino flavor transition is  $A(\nu_\alpha \rightarrow \nu_\beta) = S_{\beta\alpha}$ , where the evolution matrix  $S(x)$  satisfies the Schrödinger-like equation  $i[dS(x)/dx] = H_{\text{eff}}(x)S(x)$  with the initial condition  $S(0) = 1$ . For constant matter density, we have  $S(x) = \exp(-iH_{\text{eff}}x)$  with  $x$  being the distance that neutrinos propagate. If the evolution matrix corresponding to  $H'_{\text{eff}}$  is denoted as  $S'$ , we have  $S = U_{23}S'U_{23}^\dagger$ . The oscillation probabilities of neutrinos are given by  $P_{\alpha\beta} = |A(\nu_\alpha \rightarrow \nu_\beta)|^2 = |S_{\beta\alpha}|^2$ , while those of antineutrinos  $\bar{P}_{\alpha\beta}$  can be derived from the same effective Hamiltonian but with the replacements  $\delta \rightarrow -\delta$  and  $V \rightarrow -V$ .

As shown for example in Ref. [9], two out of nine probabilities  $P_{\alpha\beta}$  are independent. Now, we choose them as  $P_{\mu e}$  and  $P_{\mu\mu}$ . Our choice of  $P_{\mu e}$  and  $P_{\mu\mu}$  has two advantages: (1) Most of the neutrino detectors are designed for detection of electrons and muons and their antiparticles; (2) Both appearance and disappearance channels are included, which have very different sensitivities to the neutrino mass hierarchy and  $\delta$ .

We further show the dependence of  $P_{\mu e}$  and  $P_{\mu\mu}$  on  $\delta$ . Since  $S = U_{23}S'U_{23}^\dagger$ , where  $S'$  is independent of  $\theta_{23}$  and  $\delta$ , it is straightforward to prove that  $P_{\mu e}$  and  $P_{\mu\mu}$  can be written as [10, 11]

$$\begin{aligned} P_{\mu e} &= a \cos \delta + b \sin \delta + c, \\ P_{\mu\mu} &= f \cos \delta + g \cos 2\delta + h, \end{aligned} \quad (1)$$

where the relevant coefficients  $\{a, b, c\}$  and  $\{f, g, h\}$  are independent of  $\delta$  and their exact expressions can be found in Ref. [11]. Using the two independent probabilities in Eq. (1), one can readily find the exact expressions for all the other probabilities.

For neutrino oscillations in vacuum, the measure of leptonic CP violation can be taken to be the Jarlskog invariant  $\mathcal{J} \equiv s_{12}c_{12}s_{23}c_{23}s_{13}c_{13}^2 \sin \delta$ , where  $s_{ij} \equiv \sin \theta_{ij}$  and  $c_{ij} \equiv \cos \theta_{ij}$ . In fact, the difference between neutrino and antineutrino probabilities is  $P_{\alpha\beta} - \bar{P}_{\alpha\beta} \propto \mathcal{J}$  for  $\alpha \neq \beta$ . For neutrino oscillations in matter, however, the situation is complicated by the CP-asymmetric medium, since only particles rather than antiparticles are present in Earth matter. In this case, the discrepancy between  $P_{\alpha\beta}$  and  $\bar{P}_{\alpha\beta}$  receives contributions both from  $\delta$  and matter effects. Therefore, it is natural to ask which measure is the best to extract information on  $\delta$  from observations, and to find the optimal experimental setup to measure  $\delta$  in future neutrino experiments. In the literature, there already exist three distinct measures:

(i)  $A_{\alpha\beta}^{\text{CP}}(\delta) \equiv P_{\alpha\beta}(\delta) - \bar{P}_{\alpha\beta}(\delta)$  denotes the differences between neutrino probabilities  $P_{\alpha\beta}(\delta)$  and antineutrino probabilities  $\bar{P}_{\alpha\beta}(\delta)$ , where the dependence on  $\delta$  is explicitly displayed. In long-baseline experiments, where matter effects play an important role,  $A_{\alpha\beta}^{\text{CP}}(\delta)$  is no longer the

best measure of intrinsic CP violation, since  $A_{\alpha\beta}^{\text{CP}}(\delta) \neq 0$  even for  $\delta = 0$  due to matter effects. With help of the exact formula for  $P_{\mu e}$  in Eq. (1) as well as the counterpart  $\bar{P}_{\mu e}$  with coefficients  $\{\bar{a}, \bar{b}, \bar{c}\}$  in the antineutrino channel, we obtain

$$A_{\mu e}^{\text{CP}}(\delta) = \Delta a \cos \delta + \Delta b \sin \delta + \Delta c, \quad (2)$$

where  $\Delta a \equiv a - \bar{a}$ ; likewise for  $\Delta b$  and  $\Delta c$ . Obviously,  $A_{\mu e}^{\text{CP}}(\delta)$  follows the same dependence on  $\delta$  as  $P_{\mu e}(\delta)$  and  $\bar{P}_{\mu e}(\delta)$ . Note that we focus on the appearance channel  $\nu_\mu(\bar{\nu}_\mu) \rightarrow \nu_e(\bar{\nu}_e)$ , but the disappearance channel  $\nu_\mu(\bar{\nu}_\mu) \rightarrow \nu_\mu(\bar{\nu}_\mu)$  can be discussed in a similar way.

(ii)  $\Delta P_{\alpha\beta}^{\text{CP}}(\delta) \equiv P_{\alpha\beta}(\delta) - P_{\alpha\beta}(0)$  denotes the differences between the probabilities  $P_{\alpha\beta}$  for an arbitrary  $\delta$  and those for  $\delta = 0$ . This measure is intended to remove the fake CP violation induced by matter effects, which has the advantage that only the neutrino channel is involved. Using Eq. (1), we find

$$\Delta P_{\mu e}^{\text{CP}}(\delta) = 2\sqrt{a^2 + b^2} \sin \frac{\delta}{2} \sin \left( \omega - \frac{\delta}{2} \right) \quad (3)$$

with  $\tan \omega = b/a$ . It is now evident that  $\Delta P_{\mu e}^{\text{CP}}(\delta)$  is proportional to  $\sin(\delta/2)$ , and vanishes for  $\delta = 0$ .

(iii)  $\Delta P_{\alpha\beta}^{\text{m}} \equiv \max[P_{\alpha\beta}(\delta)] - \min[P_{\alpha\beta}(\delta)]$  denotes the variation of the probabilities  $P_{\alpha\beta}(\delta)$  for  $\delta$  varying in  $[0, 2\pi)$ . Such a measure is actually independent from the true value of  $\delta$ , which is yet unknown, so it should be useful to find an optimal experimental setup that is most sensitive to  $\delta$ . In fact, we have

$$\Delta P_{\mu e}^{\text{m}} = 2\sqrt{a^2 + b^2}. \quad (4)$$

Hence, one can observe that  $\Delta P_{\mu e}^{\text{m}}$  essentially determines the amplitude of  $\Delta P_{\mu e}^{\text{CP}}(\delta)$ . The basic strategy to probe  $\delta$  may first be to optimize the experimental setup with help of  $\Delta P_{\mu e}^{\text{m}}$ , and then to extract  $\delta$  from the observation of  $\Delta P_{\mu e}^{\text{CP}}(\delta)$ . In this sense,  $\Delta P_{\mu e}^{\text{m}}$  and  $\Delta P_{\mu e}^{\text{CP}}(\delta)$  can be grouped as a pair of working observables to probe  $\delta$ . Both of them are based on  $P_{\mu e}$ . Similarly, one can consider  $\Delta \bar{P}_{\mu e}^{\text{m}}$  and  $\Delta \bar{P}_{\mu e}^{\text{CP}}(\delta)$  in the antineutrino channel.

We argue that the proper measures of leptonic CP violation should manifest the difference between neutrinos and antineutrinos. In principle, most of the proposed long-baseline experiments are equally operative in the neutrino and antineutrino channels. Therefore, based on Eq. (2), we suggest a new pair of working observables:

(iv)  $\Delta A_{\alpha\beta}^{\text{CP}}(\delta) \equiv A_{\alpha\beta}^{\text{CP}}(\delta) - A_{\alpha\beta}^{\text{CP}}(0)$  signifies the intrinsic CP violation, compared to  $A_{\alpha\beta}^{\text{CP}}(\delta)$ . A similar quantity, but with a different normalization, was previously considered [12, 13]. Using the exact expression for  $A_{\mu e}^{\text{CP}}(\delta)$  in Eq. (2), we arrive at

$$\Delta A_{\mu e}^{\text{CP}}(\delta) = 2\sqrt{(\Delta a)^2 + (\Delta b)^2} \sin \frac{\delta}{2} \sin \left( \omega' - \frac{\delta}{2} \right) \quad (5)$$

with  $\tan \omega' = \Delta b/\Delta a$ . Note that this result takes the same form as that of  $\Delta P_{\mu e}^{\text{CP}}(\delta)$  in Eq. (3), except for the relevant coefficients.

(v)  $\Delta A_{\alpha\beta}^m \equiv \max[A_{\alpha\beta}^{\text{CP}}(\delta)] - \min[A_{\alpha\beta}^{\text{CP}}(\delta)]$  denotes the variation of  $A_{\alpha\beta}^{\text{CP}}(\delta)$  for  $\delta$  varying in  $[0, 2\pi)$ . The extrinsic CP-violating effects cancel in  $\Delta A_{\alpha\beta}^m$ . It is straightforward to show that

$$\Delta A_{\mu e}^m = 2\sqrt{(\Delta a)^2 + (\Delta b)^2}. \quad (6)$$

The size of  $\Delta A_{\mu e}^m$  determines the magnitude of  $\Delta A_{\mu e}^{\text{CP}}(\delta)$  through the  $\delta$ -independent coefficient.

We expect that  $\Delta A_{\alpha\beta}^{\text{CP}}$  and  $\Delta A_{\alpha\beta}^m$  can be implemented to extract  $\delta$ , and to optimize the experimental setup, similar to  $\Delta P_{\alpha\beta}^{\text{CP}}$  and  $\Delta P_{\alpha\beta}^m$ . Nevertheless, the former ones contain the difference between neutrino and antineutrino probabilities, so these two sets of measures are not equivalent. In the following, we will present approximate and analytical results for all the above measures of leptonic CP violation, and the numerical results as well. Furthermore, the optimal experimental setup for probing  $\delta$  is considered and compared with the ongoing and upcoming neutrino oscillation experiments.

### III. ANALYTICAL & NUMERICAL RESULTS

We define  $\alpha \equiv \Delta_{21}/\Delta_{31}$ ,  $\Delta \equiv \Delta_{31}L/2$  with  $L$  being the distance between the source and detector, and  $A \equiv V/\Delta_{31}$ , where  $\alpha$  denotes the ratio of the low and high oscillation frequencies,  $\Delta$  is the phase corresponding to the high oscillation frequency, and  $A$  stands for the strength of matter effects. The probabilities in matter of constant density have been calculated in Ref. [9] to the second order in both  $\alpha$  and  $s_{13}$ . According to the current neutrino oscillation data, we have  $\alpha \approx \sqrt{2}s_{13}^2 \approx 0.03$  [14–16]. Therefore, one can expand the probabilities in terms of  $\alpha$  and  $s_{13}$ , and neglect all higher-order terms of  $\mathcal{O}(\alpha^2)$ . Using the approximate formula for  $P_{\mu e}$ , we can identify the corresponding coefficients

$$\begin{aligned} a &\approx +8\alpha\mathcal{J}_r \frac{\sin A\Delta}{A} \frac{\sin(A-1)\Delta}{A-1} \cos \Delta, \\ b &\approx -8\alpha\mathcal{J}_r \frac{\sin A\Delta}{A} \frac{\sin(A-1)\Delta}{A-1} \sin \Delta, \\ c &\approx 4s_{13}^2s_{23}^2 \frac{\sin^2(A-1)\Delta}{(A-1)^2} \end{aligned} \quad (7)$$

with  $\mathcal{J}_r \equiv \mathcal{J}/\sin \delta \approx s_{13}s_{12}c_{12}s_{23}c_{23}$  being the reduced Jarlskog invariant. The coefficients  $\{\bar{a}, \bar{b}, \bar{c}\}$  for  $\bar{P}_{\mu e}$  can be obtained by replacing  $A$  with  $-A$  and  $\delta$  with  $-\delta$  in  $P_{\mu e}$ . Hence, we obtain

$$\begin{aligned} \Delta a &\approx +8\alpha\mathcal{J}_r\Theta_- \frac{\sin A\Delta}{A} \cos \Delta, \\ \Delta b &\approx -8\alpha\mathcal{J}_r\Theta_+ \frac{\sin A\Delta}{A} \sin \Delta, \\ \Delta c &\approx 4s_{13}^2s_{23}^2\Theta_+\Theta_- \end{aligned} \quad (8)$$

with  $\Theta_{\pm} \equiv \sin[(A-1)\Delta]/(A-1) \pm \sin[(A+1)\Delta]/(A+1)$ . Note that Eqs. (7) and (8) are valid as long as  $\alpha\Delta \ll 1$ ,

i.e., when the distance  $L$  and energy  $E$  are far away from the region where the low-frequency oscillation becomes dominant. This condition is satisfied in all the ongoing and upcoming long-baseline experiments, however, it is violated for atmospheric neutrino experiments. When low-frequency oscillations come into play, one can expand the probabilities in terms of  $s_{13}$ , which are exact with respect to  $\alpha$ , as is performed in Ref. [9].

Now, we apply the approximate formulas to the measures of leptonic CP violation in Eqs. (2)-(6) and explore their main features.

#### A. CP Asymmetry $A_{\mu e}^{\text{CP}}(\delta)$

From Eqs. (2) and (8), one can obtain the approximate result for  $A_{\mu e}^{\text{CP}}(\delta)$ . For neutrino energies  $E > 2$  GeV, i.e., in the high-energy approximation, we can safely ignore  $\Delta m_{21}^2$ . In this two-flavor limit,  $P_{\mu e}$  is just given by the  $\delta$ -independent term  $c$ . Note that the  $\delta$ -dependent terms arise from the interference between the two mass-squared differences, and thus are suppressed by a factor  $\alpha/s_{13}$ , indicating that the main structure of  $P_{\mu e}$  in the  $L$ - $E$  plane is determined by high-frequency and parametric resonances [7]. Given the neutrino mass hierarchy, the resonance existing in the neutrino channel should be absent in the antineutrino channel, and vice versa. For lower energies, one has to consider three-flavor oscillations and analyze the resonance structure due to  $\Delta m_{21}^2$ . For a systematic study of neutrino oscillograms of the Earth and the theoretical interpretation of their resonance structures, see Refs. [7, 8].

In Fig. 1, we have calculated  $A_{\mu e}^{\text{CP}}(\delta)$  by using the exact probabilities in the three-flavor framework and the PREM model of the Earth matter density [17]. The baseline can be calculated via  $L = 2R \cos h$  with  $R \simeq 6370$  km being the Earth radius and  $h$  the nadir angle. The abrupt transition around  $h \approx 33^\circ$  in Fig. 1 is caused by the change from the core- and mantle-crossing trajectories.

The main structure in Fig. 1 is determined by matter effects. In particular, the plots for  $\delta = 0$  indicate pure fake CP violation. In high-energy region, we have  $A_{\mu e}^{\text{CP}} \approx 4s_{13}^2s_{23}^2\Theta_+\Theta_-$  to leading order. In the neutrino channel, the high-frequency resonance exists for the normal mass hierarchy (NH). In other words,  $\sin(A-1)\Delta$  is resonantly enhanced in the NH case, while  $\sin(A+1)\Delta$  in the inverted mass hierarchy (IH). Therefore, from the NH case to the IH case,  $\Theta_-$  changes sign while  $\Theta_+$  not, which can be used to explain the sign-flipping difference between the NH and IH cases. In Fig. 1, the numerical results are presented for the NH and IH cases in the upper and lower rows, respectively. The sign-flipping difference can be clearly observed in the high-energy region. In the sub-GeV energy region, the low-frequency resonances and parametric enhancement comprise the dominant structure [8]. The peak and valley features come from the mismatch between neutrino and antineutrino probabilities. Hence, the results of  $A_{\mu e}^{\text{CP}}(\delta)$  in this re-

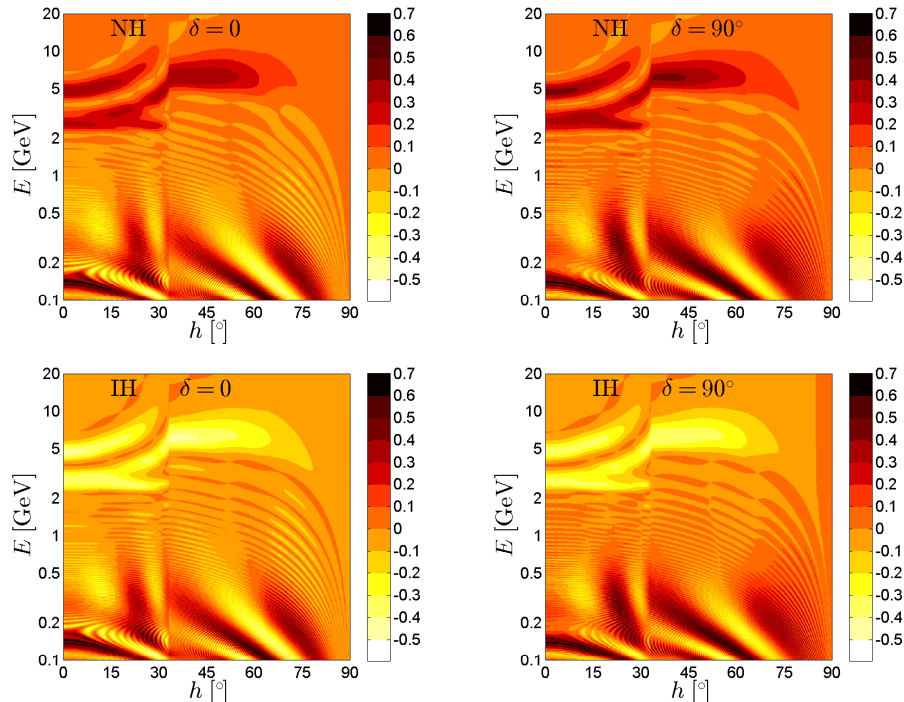


FIG. 1: Numerical results of  $A_{\mu e}^{\text{CP}}(\delta)$  for  $\delta = 0$  and  $\pi/2$  in the case of normal neutrino mass hierarchy (upper row) and inverted neutrino mass hierarchy (lower row), where the best-fit values  $\theta_{12} = 34^\circ$ ,  $\theta_{13} = 9^\circ$ ,  $\theta_{23} = 40^\circ$ ,  $\Delta m_{21}^2 = 7.5 \times 10^{-5} \text{ eV}^2$ , and  $|\Delta m_{31}^2| = 2.5 \times 10^{-3} \text{ eV}^2$  have been used [14].

gion are essentially independent of the different neutrino mass hierarchies, and tiny differences may arise from the high-order corrections of  $s_{13}$ . The difference between the two plots in each row of Fig. 1 is more evident in the low-energy region, where the condition for the high-frequency resonance is not fulfilled.

### B. Working Observables $\Delta P_{\mu e}^{\text{CP}}(\delta)$ and $\Delta P_{\mu e}^{\text{m}}$

Now, we turn to the working observables  $\Delta P_{\mu e}^{\text{CP}}(\delta)$  and  $\Delta P_{\mu e}^{\text{m}}$  based only on  $P_{\mu e}$ . Using Eqs. (3) and (7), we obtain the approximate formula

$$\Delta P_{\mu e}^{\text{CP}} = -8\alpha\mathcal{J} \frac{\sin A\Delta}{A} \frac{\sin(A-1)\Delta}{A-1} \times \left[ \tan \frac{\delta}{2} \cos \Delta + \sin \Delta \right]. \quad (9)$$

Note that the Jarlskog invariant  $\mathcal{J}$  appearing here is just a simple notation and does not mean any difference between neutrino and antineutrino oscillations. On the other hand, from Eqs. (4) and (7), we find

$$\Delta P_{\mu e}^{\text{m}} = 16\alpha\mathcal{J}_r \frac{\sin A\Delta}{A} \frac{\sin(A-1)\Delta}{A-1}. \quad (10)$$

Since both  $\Delta P_{\mu e}^{\text{CP}}(\delta)$  and  $\Delta P_{\mu e}^{\text{m}}$  have already been studied in great detail in Refs. [7, 8], we will not repeat the

analysis here. However, in Fig. 2, we have performed numerical calculations of  $\Delta P_{\mu e}^{\text{m}}$  for neutrinos and  $\Delta \bar{P}_{\mu e}^{\text{m}}$  for antineutrinos in both NH and IH cases, to illustrate the main features.

It is straightforward to understand the similarity between the case of neutrinos with NH and that of antineutrinos with IH. Note that  $\Delta P_{\mu e}^{\text{m}}$  for IH can be obtained by changing  $A \rightarrow -A$ ,  $\Delta \rightarrow -\Delta$ , and  $\alpha \rightarrow -\alpha$ . On the other hand, the formula of  $\Delta \bar{P}_{\mu e}^{\text{m}}$  for NH can be derived by replacing  $A \rightarrow -A$ . One immediately observes that these two formulas are identical. This feature is only present in the high-energy region, as shown in Fig. 2, where the similarity between the case of neutrinos with IH and that of antineutrinos with NH is also evident.

There is a resonance deep in the core region for NH. But this resonance ( $h \sim 22^\circ$  and  $2 \text{ GeV} < E < 3 \text{ GeV}$ ) disappears for IH. The oscillatory structures in the low-energy region are different for neutrinos and antineutrinos, but similar for NH and IH. Moreover, there are three vertical lines, i.e., the “solar magic lines” corresponding to  $\Delta P_{\mu e}^{\text{m}} = 0$  [8]. Solving  $\sin A\Delta = 0$ , one obtains  $A\Delta = n\pi$ , or  $L = 2n\pi/V$ , with  $n$  being a positive integer. On the other hand, the equation  $\sin(A-1)\Delta = 0$  determines the “atmospheric magic lines”. But these conditions for magic lines depend on the factorization approximation (i.e.,  $\alpha \rightarrow 0$  and  $s_{13} \rightarrow 0$ ), and the general forms can be found in Ref. [8]. In the low-energy region, the “solar magic lines” are no longer energy-independent, and they coincide with the low-frequency oscillation dips.

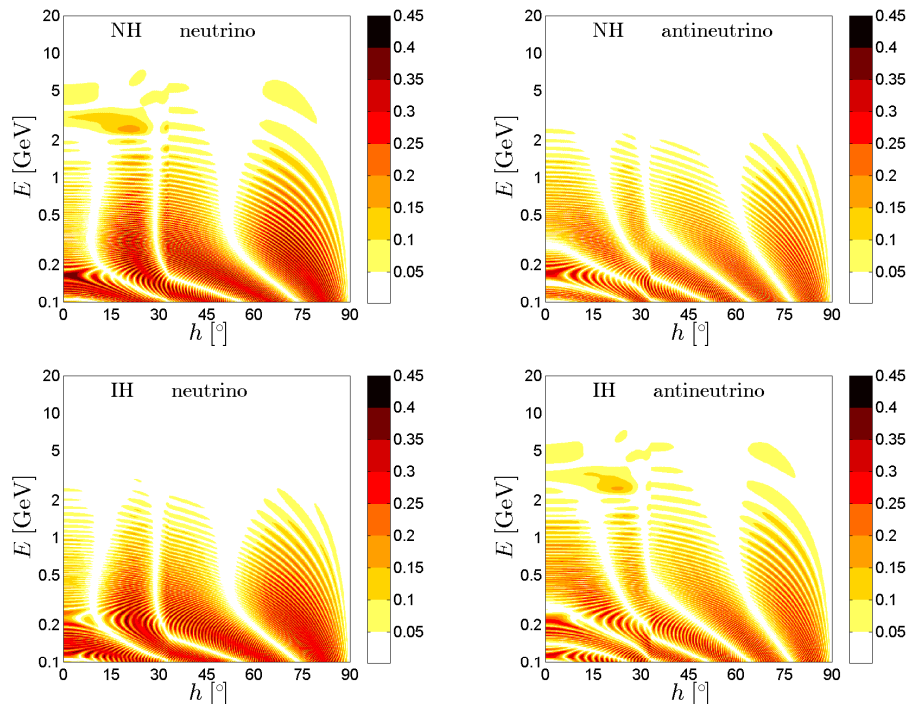


FIG. 2: Numerical results of  $\Delta P_{\mu e}^m$  and  $\Delta \bar{P}_{\mu e}^m$  in the cases of normal neutrino mass hierarchy (upper row) and inverted neutrino mass hierarchy (lower row), where the input neutrino parameters are the same as in Fig. 1.

### C. Working Observables $\Delta A_{\mu e}^{\text{CP}}(\delta)$ and $\Delta A_{\mu e}^m$

Finally, we come to the new pair of working observables  $\Delta A_{\mu e}^{\text{CP}}(\delta)$  and  $\Delta A_{\mu e}^m$ . The motivation to introduce these observables is two-fold. First, any quantity measuring leptonic CP violation in neutrino oscillations should reflect the intrinsic difference between neutrino and antineutrino probabilities. Second, it should be helpful for an optimal experimental setup to practically measure  $\delta$ . Therefore, we derive the working observables from  $A_{\mu e}^{\text{CP}}$ . Combining Eq. (5) with Eq. (8), we obtain

$$\Delta A_{\mu e}^{\text{CP}} = -8\alpha \mathcal{J} \frac{\sin A\Delta}{A} \left[ \Theta_- \tan \frac{\delta}{2} \cos \Delta + \Theta_+ \sin \Delta \right], \quad (11)$$

which reduces to the vacuum result  $A_{\mu e}^{\text{CP}}$  when  $A \rightarrow 0$ . As  $\Delta A_{\mu e}^{\text{CP}}$  is proportional to  $\mathcal{J}$ , it vanishes for  $\delta = 0$  and the CP-violating effects induced by matter effects have been removed. In Fig. 3, we show the numerical results of  $\Delta A_{\mu e}^{\text{CP}}$  for  $\delta = \pi/2$  in both NH and IH. By definition, they are just the differences between the two plots in each row of Fig. 1. Apart from a resonance region in the deep core, sizable values of  $\Delta A_{\mu e}^{\text{CP}}$  are lying in the energy region below 1 GeV. Note that the results for NH and those for IH in the high-energy region are nearly indistinguishable, which can be understood by noting that Eq. (11) is invariant under the transformations  $\alpha \rightarrow -\alpha$ ,  $\Delta \rightarrow -\Delta$ , and  $A \rightarrow -A$ .

To examine the sensitivity to  $\delta$ , we consider the range of  $A_{\mu e}^{\text{CP}}(\delta)$  by varying  $\delta$  in  $[0, 2\pi)$ . From Eqs. (6) and (8),

we find

$$\Delta A_{\mu e}^m = 16\alpha \mathcal{J}_r \sqrt{(\Theta_- \cos \Delta)^2 + (\Theta_+ \sin \Delta)^2} \frac{\sin A\Delta}{A}. \quad (12)$$

Similar to  $\Delta P_{\mu e}^m$ , the domain structure of  $\Delta A_{\mu e}^{\text{CP}}(\delta)$  and  $\Delta A_{\mu e}^m$  can be understood through the ‘‘solar’’ and ‘‘atmospheric’’ magic lines, and the interference phase condition, as suggested in Ref. [8]. In the upper (lower) row of Fig. 4, we give the numerical results of  $\Delta A_{\mu e}^m$  in NH (IH). It is now evident that the most significant value appears in the area of relatively short baselines and low energies, which are quite relevant for the long-baseline experiments. The zoom-in plots of this region are shown in the right column of Fig. 4, where the ongoing and upcoming neutrino experiments have also been indicated by solid diamonds and the energy ranges are represented by the peak energies plus error bars. It is worthwhile to mention that  $\Delta A_{\mu e}^m$  in Eq. (12) is unchanged when we switch from NH to IH through  $\alpha \rightarrow -\alpha$ ,  $\Delta \rightarrow -\Delta$ , and  $A \rightarrow -A$ . Hence,  $\Delta A_{\mu e}^m$  is insensitive to the neutrino mass hierarchy.

### D. Optimal Experimental Setup

Now, we discuss the optimal experimental setup to probe  $\delta$ . The ongoing long-baseline experiments T2K ( $E = 0.72 \pm 0.27$  GeV,  $L = 295$  km) and NO $\nu$ A ( $E = 2.02 \pm 0.43$  GeV,  $L = 810$  km), together with the proposed ones LBNE ( $E = 3.55 \pm 1.38$  GeV,  $L =$

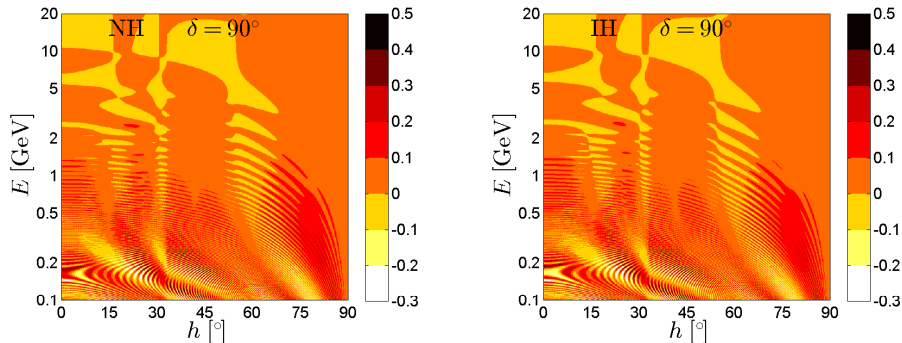


FIG. 3: Numerical results of  $\Delta A_{\mu e}^{\text{CP}}(\delta)$  for  $\delta = \pi/2$  in the cases of normal neutrino mass hierarchy (left) and inverted neutrino mass hierarchy (right), where the input neutrino parameters are the same as in Fig. 1.

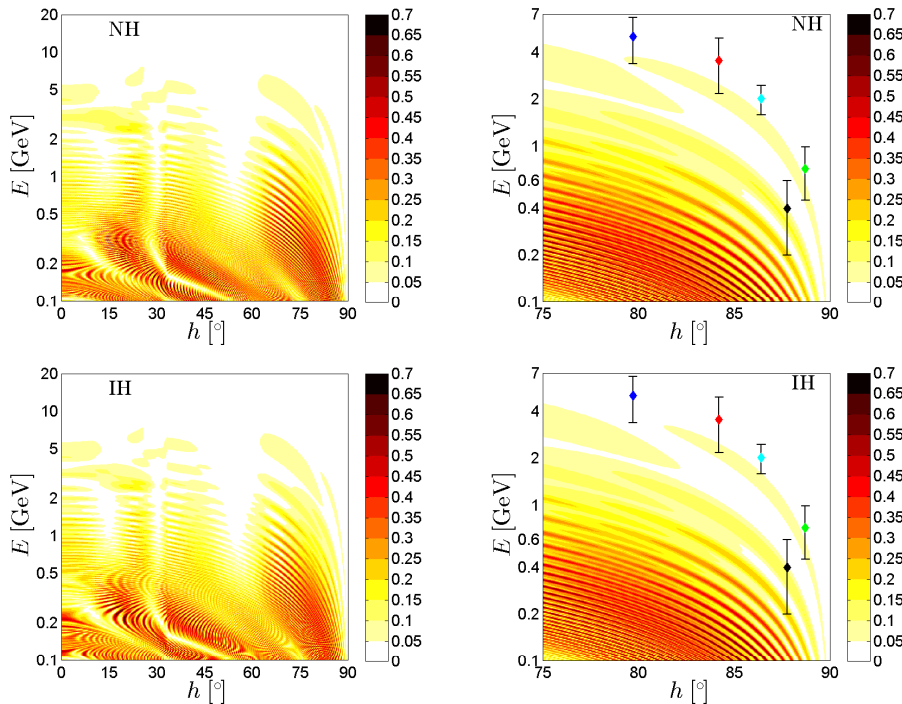


FIG. 4: Numerical results of  $\Delta A_{\mu e}^m$  in the case of normal neutrino mass hierarchy (upper row) and inverted neutrino mass hierarchy (lower row), where the input neutrino parameters are the same as in Fig. 1. In the right plots, we have zoomed in the parameter region that is relevant for the long-baseline neutrino oscillation experiments T2K (green, at  $h = 88.7^\circ$ ), NO $\nu$ A (cyan, at  $h = 86.4^\circ$ ), LBNE (red, at  $h = 84.1^\circ$ ), LAGUNA-LBNO (blue,  $h = 79.7^\circ$ ), and ESS (black, at  $h = 87.8^\circ$ ).

1300 km) and LAGUNA-LBNO<sup>1</sup> ( $E = 5.05 \pm 1.65$  GeV,  $L = 2288$  km), will be considered for illustration. Except for T2K, all experiments are intended to equally operate both in the neutrino and antineutrino channels. Therefore, one can construct the CP asymmetry  $A_{\mu e}^{\text{CP}}$  by measuring the neutrino and antineutrino probabilities. In the right column of Fig. 4, we observe that these experimental setups are lying on the “first band” (i.e.,

$\Delta A_{\mu e}^m \sim 10\%$ ), counted from top-right to bottom-left.

To improve the experimental sensitivity, one can lower the neutrino beam energy and locate the experiment on the “second band” (i.e.,  $\Delta A_{\mu e}^m \sim 15\%$ ). However, this observation is based on the probability level and we have to notice the energy dependence of the neutrino flux and the cross section. In addition, the detection efficiency and the background should be taken into account. Therefore, a detailed simulation has to be performed in order to make a final conclusion. Recently, it has been proposed that the ESS proton beam can be adjusted to produce an intense neutrino beam of energy around 0.4 GeV [18].

<sup>1</sup> At the moment, the fate of this project is unclear.

The simulation results indicate that with 8 years of data taking with an antineutrino beam and 2 years with a neutrino beam up to 73 % of the whole range of  $\delta$  could be covered at  $3\sigma$  level at the optimal baseline of around 500 km [18]. In the right column of Fig. 4, the ESS proposal is shown as  $E = 0.4 \pm 0.2$  GeV and  $L = 500$  km. Such an experimental setup happens to be on the “second band”, as we suggest. For preliminary performance of the different experimental setups, see Refs. [18–23]

It is worthwhile to mention that precision measurements of atmospheric neutrinos in the PINGU detector at the IceCube experiment on the South Pole may have good sensitivity to  $\delta$  [24]. A study of the PINGU detector and accelerator-based neutrino beams also exists [25]. On the other hand, there is no doubt that the future neutrino factories are the best place to measure  $\delta$  with high statistical significance [26–29].

#### IV. SUMMARY

We have made a complete survey of measures of leptonic CP violation in neutrino oscillation experiments. Two new working observables  $\Delta A_{\alpha\beta}^{\text{CP}}(\delta) \equiv A_{\alpha\beta}^{\text{CP}}(\delta) - A_{\alpha\beta}^{\text{CP}}(0)$  and  $\Delta A_{\alpha\beta}^{\text{m}} \equiv \max[A_{\alpha\beta}^{\text{CP}}(\delta)] - \min[A_{\alpha\beta}^{\text{CP}}(\delta)]$ , where  $A_{\mu e}^{\text{CP}}(\delta) \equiv P_{\mu e}(\delta) - \bar{P}_{\mu e}(\delta)$  is the CP asymmetry of oscillation probabilities, are suggested to describe the intrinsic leptonic CP violation. Both analytical and numerical cal-

culations are performed to illustrate their main features. The band structure of  $\Delta A_{\mu e}^{\text{m}}$  in the baseline-energy plane can be implemented to optimize the experimental setup. Furthermore, we have found that the current and future long-baseline neutrino oscillation experiments are located on the first band. On probability level, we observe that the decrease of the neutrino beam energy in a proper way could improve the experimental sensitivity.

Although the final verdict on the optimal experimental setup requires a more sophisticated simulation, we expect our analysis to be helpful in understanding the leptonic CP violation and useful in probing the leptonic CP-violating phase in future long-baseline experiments.

#### Acknowledgments

H.Z. would like to thank the Göran Gustafsson Foundation for financial support, and the KTH Royal Institute of Technology for hospitality, where this work was initiated. The authors are indebted to Evgeny Akhmedov and Mattias Blennow for useful discussions. This work was supported by the Swedish Research Council (Vetenskapsrådet), contract no. 621-2011-3985 (T.O.), the Max Planck Society through the Strategic Innovation Fund in the project MANITOP (H.Z.), and the Göran Gustafsson Foundation (S.Z.).

- 
- [1] J. Beringer et al. (Particle Data Group), *Phys. Rev.* **D86**, 010001 (2012).
  - [2] F. An et al. (Daya Bay Collaboration), *Phys. Rev. Lett.* **108**, 171803 (2012), 1203.1669.
  - [3] J. Ahn et al. (RENO collaboration), *Phys. Rev. Lett.* **108**, 191802 (2012), 1204.0626.
  - [4] L. Wolfenstein, *Phys. Rev.* **D17**, 2369 (1978).
  - [5] S. P. Mikheyev and A. Y. Smirnov, *Sov. J. Nucl. Phys.* **42**, 913 (1985).
  - [6] K. Kimura, A. Takamura, and T. Yoshikawa, *Phys. Lett.* **B640**, 32 (2006).
  - [7] E. K. Akhmedov, M. Maltoni, and A. Y. Smirnov, *JHEP* **0705**, 077 (2007), hep-ph/0612285.
  - [8] E. K. Akhmedov, M. Maltoni, and A. Y. Smirnov, *JHEP* **0806**, 072 (2008), 0804.1466.
  - [9] E. K. Akhmedov, R. Johansson, M. Lindner, T. Ohlsson, and T. Schwetz, *JHEP* **0404**, 078 (2004), hep-ph/0402175.
  - [10] K. Kimura, A. Takamura, and H. Yokomakura, *Phys. Lett.* **B537**, 86 (2002), hep-ph/0203099.
  - [11] K. Kimura, A. Takamura, and H. Yokomakura, *Phys. Rev.* **D66**, 073005 (2002), hep-ph/0205295.
  - [12] A. Donini, M. Gavela, P. Hernandez, and S. Rigolin, *Nucl. Phys.* **B574**, 23 (2000), hep-ph/9909254.
  - [13] G. Altarelli and D. Meloni, *Nucl. Phys.* **B809**, 158 (2009), 0809.1041.
  - [14] G. L. Fogli, E. Lisi, A. Marrone, D. Montanino, A. Palazzo, et al., *Phys. Rev.* **D86**, 013012 (2012), 1205.5254.
  - [15] D.V. Forero, M. Tórtola, and J.W.F. Valle, *Phys. Rev.* **D86**, 073012 (2012), 1205.4018.
  - [16] M. Gonzalez-Garcia, M. Maltoni, J. Salvado, and T. Schwetz (2012), 1209.3023.
  - [17] A. M. Dziewonski and D. L. Anderson, *Phys. Earth Planet. Interiors* **25**, 297 (1981).
  - [18] E. Baussan, M. Dracos, T. Ekelöf, E. Fernandez-Martinez, H. Öhman, et al. (2012), 1212.5048.
  - [19] K. Abe et al. (T2K Collaboration), *Nucl. Instrum. Meth.* **A659**, 106 (2011), 1106.1238.
  - [20] K. Abe et al. (T2K Collaboration), *Phys. Rev. Lett.* **107**, 041801 (2011), 1106.2822.
  - [21] M. Muether, talk given at NOW 2012, (2012).
  - [22] K. Scholberg, talk given at NOW 2012, (2012).
  - [23] A. Rubbia, talk given at NOW 2012, (2012).
  - [24] E. K. Akhmedov, S. Razzaque, and A. Y. Smirnov (2012), 1205.7071.
  - [25] J. Tang and W. Winter, *JHEP* **1202**, 028 (2012), 1110.5908.
  - [26] P. Huber, M. Lindner, and W. Winter, *Nucl. Phys.* **B645**, 3 (2002), hep-ph/0204352.
  - [27] P. Huber and W. Winter, *Phys. Rev.* **D68**, 037301 (2003), hep-ph/0301257.
  - [28] S. K. Agarwalla, P. Huber, J. Tang, and W. Winter, *JHEP* **1101**, 120 (2011), 1012.1872.
  - [29] P. Coloma, P. Huber, J. Kopp, and W. Winter (2012), 1209.5973.